environmental microbiology

Environmental Microbiology (2010) **12**(4), 990–1000 doi:10.1111/j.1462-2920.2009.02143.x

A new group of cosmopolitan bacteriophages induce a carrier state in the pandemic strain of *Vibrio parahaemolyticus*

Roberto Bastías, Gastón Higuera, Walter Sierralta and Romilio T. Espejo*

Instituto de Nutrición y Tecnología de los Alimentos, Universidad de Chile, Santiago, Chile.

Summary

A clonal population of pathogenic *Vibrio parahaemolyticus* O3 : K6 serovar has spread in coastal waters, causing outbreaks worldwide since 1996. Bacteriophage infection is one of the main factors affecting bacterial strain concentration in the ocean. We studied the occurrence and properties of phages infecting this *V. parahaemolyticus* pandemic strain in coastal waters. Analysing 143 samples, phages were found in 13. All isolates clustered in a closely related group of podophages with at least 90% nucleotide sequence identity in three essential genes, despite distant geographical origins. These bacteriophages were able to multiply on the *V. parahaemolyticus* pandemic strain, but the impact on host concentration and subsequent growth was negligible. Infected bacteria continued producing the phage but were not lysogenized. The phage genome of prototype strain VP93 is 43 931 nucleotides and contains 337 bp direct terminal repeats at both ends. VP93 is the first non-*Pseudomonas* phage related to the ΦKMV-like subgroup of the T7 supergroup. The lack of a major effect on host growth suggests that these phages exert little control on the propagation of the pandemic strain in the environment. This form of phage growth can be modelled if phage-sensitive and -resistant cells that convert to each other with a high frequency are present in clonal cultures of pandemic *V. parahaemolyticus*.

Introduction

Bacteriophages are highly abundant in the oceans, where they contribute to host mortality and play an important role in shaping the abundance and diversity of marine bacteria (Wommack and Colwell, 2000; Suttle, 2005; Brussaard *et al*., 2008). Bacteriophages also likely play a role in the occurrence of diarrhoea outbreaks caused by *Vibrio parahaemolyticus*, a marine bacterium that causes severe diarrhoea when present in seafood in infective doses. The most probable relevant role of phages is reducing the bacterial load by killing the bacteria (Bouvier and Giorgio, 2007), although they can also modify fitness (Zabala *et al*., 2009) or intervene in evolution by lysogenic conversion and lateral transfer (Brüssow *et al*., 2004). *Vibrio parahaemolyticus* is a diverse population common in various locations of the littoral, including a minor fraction of pathogenic strains (Depaola *et al*., 2000; Alam *et al*., 2003; Hara-kudo *et al*., 2003; Depaola *et al*., 2003a,b; Fuenzalida *et al*., 2006). Among the pathogenic strains, a particular group that is clonal in nature and originally observed in Bangladesh in 1996 has spread worldwide, becoming the first known pandemic of *V. parahaemolyticus* (Nair *et al*., 2007). At least 65 genes are specifically present in the pandemic strains compared with the non-pandemic strains, including several genes related to pathogenicity in a 80 kb island containing two haemolysin (*tdh*) genes and a set of genes for the type III secretion system (Izutsu *et al*., 2008). Bacteriophages, which play a major role in bacterial genomic diversity, may generate variants of this strain (Ogura *et al*., 2006).

Bacteriophages that infect and kill different strains of *V. parahaemolyticus* have been reported, but there have been no surveys of lytic phages able to infect the pandemic strain. The abundance of phages against *V. parahaemolyticus* in inshore marine animals (Baross *et al*., 1978) and the abundance and genetic richness of vibriophages in oysters and seawater were recently reported (Comeau *et al*., 2005; 2006). Vibriophages are found in samples of oysters and water at a concentration of 10^4 viruses cm^{-3} and less than 1 l^{-1} respectively. Most isolates corresponded to *Siphoviridae*, followed by *Podoviridae*.

A fair number of *V. parahaemolyticus* phages have been isolated and characterized in greater detail. VpV262, which has a 46 012 bp genomic sequence, is probably a distant relative of T7 (Hardies *et al*., 2003). The complete genome sequence of the T4-like, broad-host-range vibriophage KVP40 has also been determined

Received 11 August, 2009; accepted 26 November, 2009. *For correspondence. E-mail romilio.espejo@gmail.com; Tel. (+56) 2 9781426; Fax (+56) 2 2214030.

(Miller *et al*., 2003). All *V. parahaemolyticus* phages, except a few filamentous phages of the *Inoviridae* family, belong to the three families of tailed phages: *Myoviridae*, *Siphoviridae* and *Podoviridae*. These phages are generally species-specific and sometimes strain-specific, although a few demonstrate a broader host range against *Vibrio* and the related genus *Photobacterium* (Matsuzaki *et al*., 2000). Phages against *V. parahaemolyticus* also have been used for typing strains of this species (Kudriakova *et al*., 1992); however, they have not been commonly employed due to an apparent lack of specificity. Temperate phages have been isolated from *V. parahaemolyticus* using mitomycin C and ultraviolet light as inducing agents (Ohnishi and Nozu, 1986; Koga and Kawata, 1991); one study found that 10% of *V. parahaemolyticus* isolates harbour lysogens (Muramatsu and Matsumoto, 1991). Two of the recovered phages have been shown to be generalized transducing phages.

Only three temperate phages have been associated with the pandemic strain. The temperate *Inoviridae* phage f237 is found integrated in most bacterial pandemic isolates providing its characteristic orf8, an open reading frame (ORF) used as a marker of pandemic strains (Nasu *et al*., 2000; Iida *et al*., 2001). Two other temperate myovirus phages were recently reported (Lan *et al*., 2009; Zabala *et al*., 2009); both belong to a fairly new group of telomeric phages. One of these phages enhances the UV sensitivity of the lysogenized host and may play a significant role in reducing the survival and propagation capability of the *V. parahaemolyticus* pandemic strain in the ocean (Zabala *et al*., 2009). We explored the existence of lytic phages for the pandemic strain in an initial effort to asses their potential role in the survival of the pandemic strain. We found a single cosmopolitan phage group in widely separated geographical locations. These phages replicate in the pandemic *V. parahaemolyticus* strain without evident harm and can be co-cultured with its host, although they do not lysogenize the cells. We present a possible mechanism for such phage replication.

Results

The presence in finfish and shellfish of phages infecting *V. parahaemolyticus* pandemic clonal complex isolates was determined in samples from different geographic locations. Phages in the samples were enriched by incubation in liquid cultures of the pandemic strain PMC 57.5 and tested for the formation of plaques on the same bacteria. The PMC 57.5 strain was an isolate chosen as a type strain of the pandemic *V. parahaemolyticus* isolates obtained in Chile (Fuenzalida *et al*., 2006). Plaque-forming units (pfu) were observed in 13 of 143 enrichments from different samples (Table 1). Positive samples were found in every examined region except Antofagasta.

General characterization of V. parahaemolyticus *phage isolates*

Bacteriophage clones obtained from single plaques were grown, partially purified, and differentiated based on their morphology and nucleic acid properties. Only one plaque per sample was analysed. The 13 isolates were resistant to chloroform and their nucleic acid consisted of double-stranded DNA, as indicated by sensitivity to DNase I and DNA restriction enzymes, and by resistance to RNase A. After pulsed field gel electrophoresis, the DNAs of the 13 isolates migrated with an apparent size of 42 kb. Nine different isolates were observed under the electron microscope; all corresponded to *Podoviridae* or podophages and consisted of icosahedral particles 45 nm in diameter with a short 10-nm-long tail (Fig. 1). No morphological differences were evident

Table 1. Bacteriophages against *V. parahaemolyticus* pandemic clone PMC 57.5 isolated from shellfish and finfish obtained in Chile and Mexico.

Origin (No. positive/No. negative)	Isolate	Isolation date	Sample	Isolation place	RFLP group[a]
Región de Los Lagos Chile (8/123)	5090	30/8/2005	Clams	Cailín,	D
	5093	30/8/2005	Clams	Yelcho	D
	5489	13/9/2005	Clams	Yelcho	D
	5312	5/9/2005	Clams	Yelcho	A
	5486	13/9/2005	Clams	Isla Chulín,	C
	6119	12/10/2005	Clams	Golfo Ancud	D
	7860	27/12/2005	Clams	Coronel, B-B	D
Puerto Progreso, Mexico (4/6)	5e	11/8/2005	Finfish digestive tract	Puerto Progreso	B
	2e	11/8/2005	Robalo digestive tract		D
	4e	11/8/2005	Mojarra digestive tract		D
	6e	11/8/2005	Oyster		E
Acapulco (2/10)	512	24/4/2007	Oyster	Acapulco Bay	F
	1032	24/4/2007	Small black clam		G

a. RFLP obtained using HaeIII.

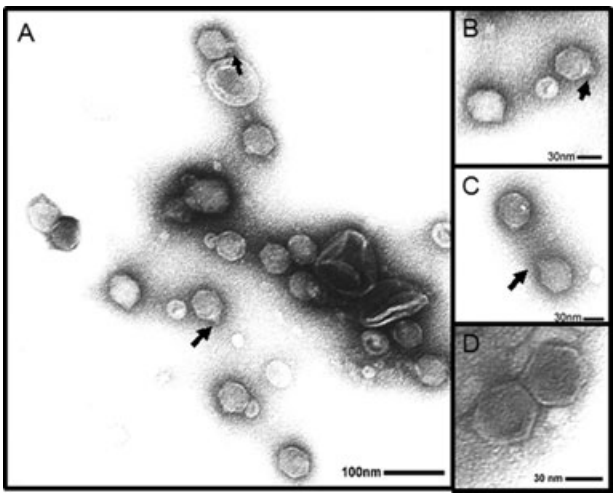

Fig. 1. Electron microscopy of phages infecting *V. parahaemolyticus* pandemic strain PMC 57.5 negatively stained with uranyl acetate. Arrows indicate a tail. A and B correspond to isolate VP93; C and D correspond to isolates 5e and 5312 respectively.

between the nine isolates. The restriction fragment length polymorphism (RFLP) of the phage DNAs obtained with HaeIII allowed for seven groups to be distinguished (Fig. 2 and Table 1). Seven isolates clustered in group D despite some being obtained from distant geographical locations (for example, see 4e from Mexico and 5093 from Chile). Phylogenetic relationships were also examined by similarities in putative genes for DNA and RNA polymerases and exonuclease (GenBank Accession No. FJ896201–FJ896221). Only two group D isolates were included in the characterization. Isolates differentiated by their RFLP patterns were also differentiated by the sequence of their three genes together, except for isolate 6e, which made a single group with the two group D isolates (Fig. S1).

Growth of phages on V. parahaemolyticus

Isolate 5093, which belongs to the most abundant RFLP cluster and is hereafter called VP93, was chosen for detailed characterization. VP93 and other phages from different RFLP clusters were able to infect different strains of pandemic and non-pandemic *V. parahaemolyticus*. Interestingly, the phages did not infect all strains belonging to the pandemic clonal group, indicating diversity within the group (Table S1). Plaques observed after titrating VP93 and the rest of the isolates were consistently turbid, independent of the host *V. parahaemolyticus* strain. The phage plaques were observed only during a brief period, between 2 and 3 h of incubation, because they rapidly disappeared after further incubation. A similar observation was made after infection in liquid culture. Only a slight decrease in the bacterial growth rate was observed after infection in liquid medium, and the normal growth rate rapidly recovered, even at a multiplicity of 10 pfu per cell (Fig. 3A). Although cell lysis was not observed, phage production of approximately 100 pfu per total cell present at the time of infection was calculated. The successive cloning of host strains to surmount the potential presence of resistant cells did not change these results. Attempts to isolate sensitive and resistant clones from independent colonies were unsuccessful. Of 300 colonies assayed, none were found to be significantly more sensitive than the original culture. The presence of a high proportion of naturally resistant cells was confirmed by determining the colony-forming units (cfu) in the permanent presence of phage; a variable proportion of 50–90% of the cfu obtained in the absence of phage was observed, depending on the origin and stage of the culture. When VP93-infected bacterial cultures were serially cultured after 1/100 dilution, bacteria grew as well as in non-infected cultures, although the phage persisted in the cultures at approximately 1 pfu per cell (Fig. 3B). Per-

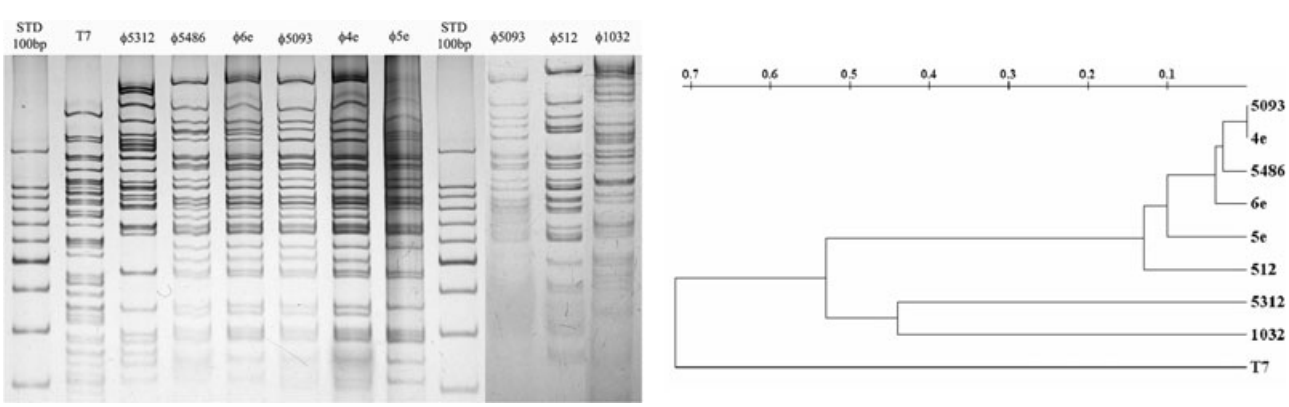

Fig. 2. Restriction fragment length polymorphism (RFLP) pattern of pandemic *V. parahaemolyticus* PMC 57.5 phage isolates obtained from finfishes and shellfishes from Chile and México. Right: A dendrogram illustrating the pattern clusters by dissimilarity. Isolates 5090, 5489, 6119, 7860 and 2e showed RFLP identical to 5093 and 4e, and they are not shown.

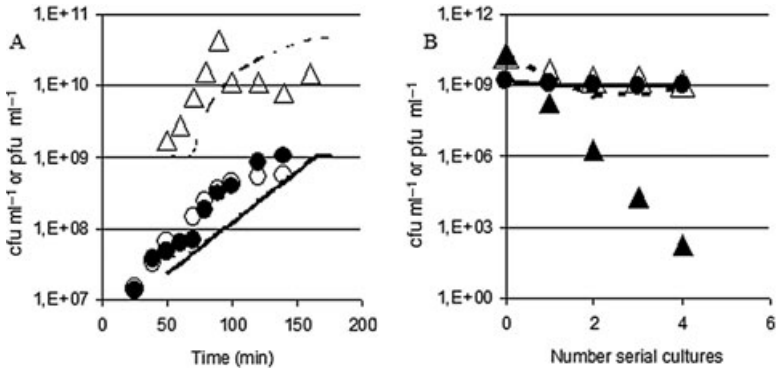

Fig. 3. Growth of VP93 in pandemic *V. parahaemolyticus*.
A. Plaque-forming units (△), cfu (●) and total bacteria calculated from the absorbance (○) after infection of PMC 57.5 with VP93 at moi 10. Lines represent the numbers for pfu, cfu and total cells estimated according to the model based on the existence of resistant and sensitive bacteria in the same bacterial clone, described in *Experimental procedures*.
B. Plaque-forming units (△) and cfu (●) observed after infection, and after the indicated number of subsequent serial cultures of the infected cells upon 1/100 dilution; (▲) indicates the pfu expected after each serial dilution if the phage does not replicate. Continuous and discontinuous lines show estimated cfu and pfu, respectively, according to the model based on the existence of resistant and sensitive bacteria in the same bacterial clone described in *Experimental procedures*.

sistence after five serial 1/100 dilutions indicated that the phage reproduced in these cultures; otherwise, it should have been diluted out (black triangle, Fig. 3B). The persistence of VP93 due to lysogeny was ruled out by the absence of phage genes in colonies of bacteria growing after phage infection. When 20 colonies obtained from infected cultures and purified by two serial cultures in solid medium were examined by PCR amplification, none were positive for the putative RNA and DNA phage polymerase genes of VP93 (see *Experimental procedures* for details). Additionally, mitomycin C treatment failed to induce phage production in cells from the 20 colonies.

Persistence of VP93 in infected cultures

Thorough washing of the cells growing together with VP93 did not eliminate all pfu; approximately 1% remained with the cells. These phages could be either inside productively infected cells or tightly associated with the bacteria. Our overall observations of VP93 growth can be explained by the presence of two cell types, sensitive and resistant, at similar concentrations in the original culture, even in recently cloned cultures. This observation would result if resistant and sensitive cell types turn into each other at similar, high rates. One possible mechanism could be phase variation. Upon infection, sensitive cells produce phages and die, but the growth of resistant cells continues unaffected. These resistant cells would, however, generate sensitive cells that can be infected by the phage, maintaining phage growth and precluding its dilution upon serial dilution and culturing. Assuming this situation, the bacterial and bacteriophage population dynamics were modelled on the equations and computer calculations described by Levin and Bull (2004). Discontinuous lines in Fig. 3A and B show the expected values if VP93 had a burst size of 1000 with a latent period of 18 min and the host bacteria changed from sensitive to resistant or vice versa at a rate of 0.01 per generation. This change could occur by phase variation. Because *V. parahaemolyticus* undergoes phase variation between opaque (op) and translucent (tra) colony morphologies (Enos-Berlage and McCarter, 2000), we explored the possible relationship between phage resistance and the op and tra colony types. No significant differences in resistance were observed between the op and tra colonies; both contained 50–90% resistant cells.

VP93 genome

The VP93 genome was sequenced using a combination of the shotgun and primer walking approaches (GenBank Accession No. FJ 896200). The genome was 43 931 nucleotides long with a G+C content of 49.2%, 3.8% higher than the G+C content of the host (Makino *et al.*, 2003). Direct terminal repeats (DTRs) 337 bp in length were observed at the ends. The DTRs were confirmed by primer walking, but the ends could not be exactly defined due to the absence of a clear abrupt stop when sequencing the end regions.

The phage could not be ascribed by nucleotide sequence similarity to any known phage group. However, the genome contained 44 putative ORFs based on Artemis analysis (Rutherford *et al.*, 2000) and 16 of their putative products (39%) shared significant similarities with proteins of the ΦKMV subgroup of the T7 supergroup, composed of *Pseudomonas* phages ΦKMV, LKD16, LKA1 and LUZ19 (Ceyssens *et al.*, 2006). These genes correspond to DNA metabolism, structural proteins and

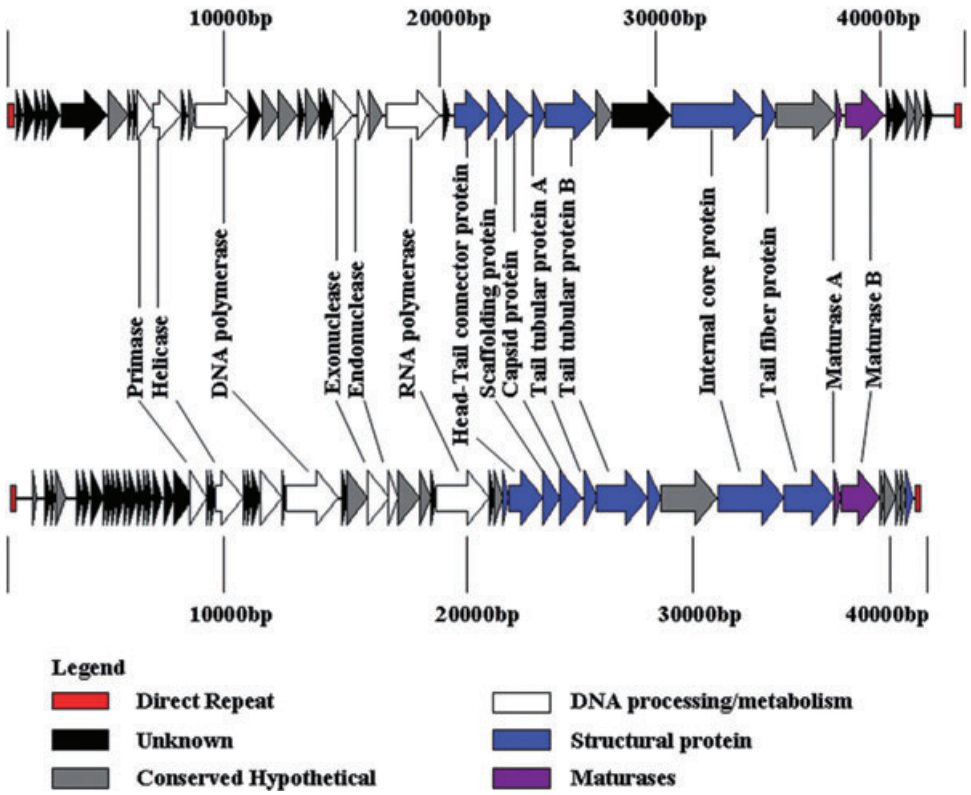

Fig. 4. Genomic map of VP93 and LKA1, the closest phage within the ΦKMV subgroup of the T7 supergroup. Patterns were assigned based on functional assignments of the ORFs as indicated in the key. The LKA1 map was based on the sequence with Accession No. AM265639.

maturase proteins. The genome organization is also very similar to phages of this group (Fig. 4 and Table 2); it contains two functional genomic regions. The first region (early genes) encompasses a set of unknown genes probably involved in host conversion, DNA replication and RNA polymerase. The second region (late genes) comprises genes coding for structural and potential lysis proteins, like glycosyl hydrolase. According to this organization, most of the non-conserved ORFs observed in the VP93 sequence correspond to genes coding for host conversion and lysis at the start of the early region and at the end of the late region respectively. An ORF with similarity to DNA ligase, common in the ΦKMV subgroup, was not found in the VP93 genome.

The RNA polymerase protein has a high degree of similarity to phage T7 (BLAST *E*-value 6e-49; 25% identity). Other proteins were exclusively related to those found in the ΦKMV subgroup. RNA polymerase exhibits high conservation with the phages of the subgroup and T7 for the region around the essential catalytic residues. The recognition and specificity loops, which interact with the T7-like phage promoters, are strongly divergent from T7 but share some similarity with the phages of the subgroup. These two regions are more conserved with LKA1 than ΦKMV and LKD16 (Table S2).

Discussion

We explored the existence of lytic phages for the *V. parahaemolyticus* pandemic strain in an effort to assess their potential role in the survival of the pandemic strain in the environment. The lack of a major effect of this phage on host growth suggests that it and the related phage group exert little control on the propagation of the pandemic strain in the environment. Our finding that every phage isolate for the *V. parahaemolyticus* pandemic strain corresponds to a single cohesive group despite distant geographical origins seems exceptional. Interestingly, KVP40, a *V. parahaemolyticus* lytic phage with a wide host range (Miller *et al.*, 2003), was not detected in our study. This phage produces clear plaques, results in liquid culture clearing, and very little resistance remains after infection of the pandemic strain (data not shown). On the other hand, almost identical phages in distant geographical regions were previously reported; bacteriophages ΦKMV and LKD16, for example, were isolated from water samples from Russia and Belgium, respectively, and have 90% DNA homology (Ceyssens *et al.*, 2006).

One of the more interesting properties of bacteriophage VP93 is its capacity to multiply on the *V. parahaemolyticus* pandemic strain without an evident effect on its growth.

Table 2. ORFs of the VP93 genome and BLAST hits.

ORF	Nucleotide position	Predicted function	Related BLAST hits (Accession No.; *E*-value)
7	4 619–5 521	Peptidase	Hypothetical protein Sala_2518 *Sphingopyxis alaskensis* RB2256 (YP_617558.1; 2e-14); metal-dependent hydrolase *Thermus* phage (P23-45 YP_001467909.1; 1e-13)
10	5 916–6 728	Primase	Primase *Pseudomonas* phage LUZ19 (YP_001671958.1; 3e-18); putative DNA primase *Pseudomonas* phage LKA1 (YP_001522861.1; 6e-17)
11	6 710–7 990	Helicase	Putative DNA helicase *Pseudomonas* phage LKA1 (YP_001522864.1; 2e-85); putative DNA helicase *Pseudomonas* phage LKD16 (YP_001522805.1; 1e-70)
13	8 349–8 654	Hypothetical protein	Hypothetical protein PPLUZ24_gp30 *Pseudomonas* phage LUZ24 (YP_001671903.1; 1e-11); protein 7.7 *Yersinia pestis* phage phiA1122 (NP_848293.1; 1e-07)
14	8 651–11 086	DNA polymerase	Putative DNA polymerase *Pseudomonas* phage LKA1 (YP_001522870.1; 0); DNA polymerase *Pseudomonas* phage LUZ19 (YP_001671963.1; 0)
17	12 481–13 296	Hypothetical protein	Hypothetical protein PPLKA1_gp31 *Pseudomonas* phage LKA1 (YP_001522872.1; 5e-31); hypothetical protein PPLKD16_gp21 *Pseudomonas* phage LKD16 (YP_001522812.1; 3e-29)
19	13 687–14 316	Hypothetical protein	Hypothetical protein CGSHiII_06933 *Haemophilus influenzae* PittII (ZP_01795538.1; 1e-19); hypothetical protein *Pseudomonas* phage 14-1 (YP_002364358.1; 3e-16)
22	14 957–15 907	Exonuclease	Putative DNA exonuclease *Pseudomonas* phage LKA1 (YP_001522873.1; 1e-61); putative exonuclease *Pseudomonas* phage PT2 (YP_002117805.1; 4e-61)
23	16 087–16 527	Endonuclease	Putative DNA endonuclease *Pseudomonas* phage LKA1 (YP_001522874.1; 9e-28); putative DNA endonuclease VII *Pseudomonas* phage LKD16 (YP_001522814.1; 2e-25)
24	16 643–17 227	Hypothetical protein	Phage protein *Enterobacteria* phage phiEcoM-GJ1 (YP_001595438.1; 6e-24); ATP-binding protein *Enterobacteria* phage phiEco32 (YP_001671779.1; 8e-20)
25	17 413–19 863	RNA polymerase	Putative RNA polymerase *Pseudomonas* phage LKA1 (YP_001522878.1; 5e-99); putative DNA-dependent RNA polymerase *Pseudomonas* phage phiKMV (NP_877465.1; 8e-97)
27	20 555–22 087	Head–tail connector protein	Head–tail connector protein *Pseudomonas* phage PT2 (YP_002117815.1; 8e-89); putative head–tail connector protein *Pseudomonas* phage LUZ19 (YP_001671975.1; 1e-88)
28	22 087–22 902	Scaffolding protein	Putative scaffolding protein *Pseudomonas* phage LKA1 (YP_001522883.1; 1e-07); putative scaffolding protein *Pseudomonas* phage LKD16 (YP_001522823.1; 3e-06)
29	22 967–23 965	Capsid protein	Predicted capsid protein *Escherichia coli* O127 : H6 str. E2348/69 (YP_002332050.1; 3e-66); capsid protein *Pseudomonas* phage phiKMV (NP_877471.1; 2e-59)
30	24 171–24 731	Tail tubular protein A	Tail tubular protein A *Pseudomonas* phage LUZ19 (YP_001671978.1; 4e-20); putative tail tubular protein A *Pseudomonas* phage LKD16 (YP_001522825.1; 6e-20)
31	24 741–27 083	Tail tubular protein B	Putative tail tubular protein B *Pseudomonas* phage LKA1Y(P_001522886.1; 8e-91); putative tail tubular protein B *Pseudomonas* phage LKD16 (YP_001522826.1; 2e-74)
34	30 577–34 431	Internal core protein	Internal core protein *Pseudomonas* phage phiKMV (NP_877476.1; 7e-25); putative internal core protein *Pseudomonas* phage PT5 (YP_002117763.1; 1e-24)
35	34 750–35 361	Tail fibre protein	Putative tail fibre protein *Pseudomonas* phage LKD16 (YP_001522830.1; 2e-04); putative tail fibre protein *Pseudomonas* phage PT5 (YP_002117764.1; 3e-04)
36	35 370–38 102	Glycosyl hydrolase	*O*-glycosyl hydrolase, family protein *Acholeplasma laidlawii* PG-8A (YP_001621049.1; 1e-23); endo-beta-1,3-1,4 glucanase *Pedobacter* sp. BAL39 (ZP_01886294.1; 1e-15)
37	38 112–38 411	DNA maturase A	Putative DNA maturase A *Pseudomonas* phage LKA1 (YP_001522891.1; 1e-07); putative DNA maturase A *Pseudomonas* phage LKD16 (YP_001522834.1; 2e-04)
38	38 536–40 341	DNA maturase B	Putative DNA maturase B *Pseudomonas* phage PT5 (YP_002117769.1; 8e-145); putative DNA maturase B *Pseudomonas* phage phiKMV (NP_877482.1; 3e-144)
41	41 347–41 760	Hypothetical protein (peptidase)	Gp46 *Enterobacteria* phage SP6 (NP_853606.1; 2e-13); peptidase M15A *Desulfotomaculum reducens* MI-1 (YP_001111881.1; 4e-13)
42	41 753–42 121	Hypothetical protein	Hypothetical protein Mext_2445 *Methylobacterium extorquens* PA1 (YP_001639911.1; 6e-18); hypothetical protein epsilon15p50 *Enterobacteria* phage epsilon15 (YP_850991.1; 4e-16)

BLAST *E*-values below 10^{-3} were considered non-significant.
The following ORFs did not have significant hits: 1 (42–306), 2 (258–795), 3 (895–1207), 4 (1217–1367), 5 (1447–2029), 6 (2069–4211), 8 (5134–5314), 9 (5369–5534), 12 (7607–7850), 15 (10 718–11 293), 16 (11 302–11 895), 18 (12 959–13 291), 20 (13 932–14 135), 21 (14 145–14 570), 26 (19 917–20 162), 32 (27 093–27 839), 33 (24 357–27 455), 39 (40 062–40 361), 40 (40 370–40 954), 43 (41 855–42 187) and 44 (42 232–42 324).

The persistence of VP93 without an effect on bacterial growth is not likely due to lysogenic conversion because no traces of phage genes were found in resistant bacteria. The persistence of non-temperate phages in liquid cultures of bacteria is not uncommon. The phenomenon has been called the carrier state, chronic infection and pseudolysogeny, which also has different definitions. No common explanation exists for all of these observations, and they could occur by very different mechanisms (Barksdale and Arden, 1974). A likely explanation for our observations is that phage persistence was due to the occurrence of two cell types, sensitive and resistant, at similar concentrations, even in recently cloned cultures. This situation could occur if resistant and sensitive cell types become the other cell type at high rates. Based on this assumption, the observed results were reproduced by

a model incorporating the following parameters: burst size of 1000, latent period of 18 min, phage adsorption rate of 10^{-8}, and a conversion rate of sensitivity to resistance and vice versa of 0.01 per generation. The latent period and adsorption rate correspond to the experimentally obtained values. A burst size of 1000 was assumed from the yield of phage per total bacteria in the culture, considering that only 10% of the cells are sensitive (Fig. 3A). The conversion rate for host sensitivity was arbitrary, assuming that it could occur by phase transition. The failure to find a relationship between phage resistance and colony type does not rule out resistance and sensitivity occurring by phase variation not associated with the op and tra character. The failure to isolate sensitive and resistant clones from colonies can be explained by high resistance/sensitivity variation. However, this result would be expected if the rate of change from resistant cell to sensitive cell and from sensitive cell to resistant cell occurs at a frequency of 0.01 per generation. In such colonies, even those derived from a single resistant or sensitive cell, both types of cells would be present. The modulation of phage infection by phase variation was previously described in *Streptomyces coelicolor* (Sumby and Smith, 2003) and *Haemophilus influenzae* (Zaleski *et al*., 2005).

Bacteriophage PPO1, which stably coexists with *Escherichia coli* O157 : H7-like VP93 without lysogenic conversion, is explained by clonal heterogeneity of the host (Fischer *et al*., 2004). This phenomenon is not unique; similar observations were later reported with phages of *Salmonella* spp. (Carey-smith *et al*., 2006) and *Flavobacterium psychrophilum* (Middelboe *et al*., 2009). In all of these cases, the chosen explanation was that only a subpopulation of the host is susceptible to phage infection, but the cause of the presence of this subpopulation was not explained. The carrier state in co-habitation as described here, or the replication of the phage without hurting the host, seems to be advantageous for the persistence of both the phage and bacteria in close proximity. Importantly, because phages are isolated or detected by plaque formation, phages that grow without harming their hosts could occur more frequently in nature than reported due to difficulty observing plaques in such cases. This phage–bacteria relationship generates a phenomenon analogous to what happens with 'non-cultivable' bacteria; phages like VP93 are not readily detectable unless they have another host available for detection that they can lyse with good efficiency. Some of these phages may correspond to the large number of putative phages observed in culture-independent studies, but without any cultured representative (Breitbart and Rohwer, 2005).

The sequence of VP93 showed that it is related, though distantly, to the ΦKMV subgroup of phages and it is the first non-*Pseudomonas* phage present in this subgroup. Among the phages in this subgroup VP93 is more closely related to phage LKA1. We found no similarity between VP93 and VpV262, a marine bacteriophage VpV262, which infects *V. parahaemolyticus*, included in the T7 supergroup in spite of lacking RNA polymerase (Hardies *et al*., 2003).

Experimental procedures

Strains and growth media

Vibrio parahaemolyticus strain PMC 57.5 was previously characterized (Fuenzalida *et al*., 2006). Bacteria and phage were grown in synthetic sea water (23.4 g l^{-1} NaCl, 24.7 g l^{-1} $MgSO_4 \cdot 7H_2O$, 1.5 g l^{-1} KCl and 1.43 g l^{-1} $CaCl_2 \cdot 2H_2O$, pH 6.5) supplemented with 1% Bacto tryptone (Gifco) and 0.5% yeast extract at 37°C with reciprocal shaking.

Bacteriophage isolation and characterization

Shellfish and finfish were collected in the coastal waters of the Pacific Ocean off Chile, Region de los Lagos, next to Puerto Montt (41°29′S, 72°24′W) and Antofagasta (23°39′S, 70°24′W), and off Mexico, next to Acapulco, Guerrero (16°51′N, 99°52′W) and Puerto Progreso, Yucatán (21°18′N, 89°39′W). The fish were kept on ice immediately after collection and processed in the laboratory within 4 h. The soft meat of the shellfish or the digestive tract of the finfish was macerated and resuspended in an equal volume of PBS buffer (NaCl 0.8%, KCl 0.02%, Na_2HPO_4 0.14%, KH_2PO_4 0.024%) and subsequently centrifuged at 5000 *g* for 10 min. Supernatant (100 μl) was then used to inoculate an exponentially growing PMC 57.5 culture of ~10^8 cells per ml and incubated overnight at 37°C with agitation. The culture was pelleted by centrifugation at 5000 *g* for 10 min and the remaining bacteria were removed by filtering (0.22 μm). Phages in the filtrate were detected by plating 100 μl using the standard method for double-layer agar plaque assay. One plaque was picked from each positive sample and re-plated two times to ensure clonal phage stocks.

For phage growth, 50 ml of a *V. parahaemolyticus* PMC 7.5 culture (~10^8 cells per ml, optical density 0.2–0.3 at 600 nm) was infected at a multiplicity of infection (moi) of 10 and incubated overnight. The culture was centrifuged at 5000 *g* for 10 min and the supernatant filtrated (0.22 μm) and combined with 10 μl of chloroform. Alternatively, strain PMA112, obtained from shellfish, was used as an indicator strain. For electron microscopy, this preparation was centrifuged at 100 000 *g* for 50 min and the pellet suspended in 100 μl of synthetic sea water. Samples were stained with 1% uranyl acetate on grids with carbon-stabilized formvar and observed using a Phillips CM 100 transmission electron microscope. Only nine isolates were observed: 5090, 5093, 5489, 5312, 5486, 1032, 512, 5e and 2e. Phage DNA was extracted from infected cultures that were centrifuged and filtered as described above, but in this case the phages in the filtrate were precipitated with polyethyleneglycol (PEG-8000) and NaCl at a final concentration of 10% and 1.5 M respectively. The precipitated phage was then centrifuged at 11 000 *g* for 20 min and suspended in synthetic sea water. For DNA extraction, samples were incubated with DNase (2 μg ml^{-1})

and RNase (100 μg ml^{-1}) for 1 h at 37°C. These samples were subsequently treated with 500 μg ml^{-1} proteinase K for 15 min at 65°C. Sodium dodecyl sulfate (SDS) was added at a final concentration of 0.5% (w/v). After incubation at 65°C for 45 min, the solution was extracted twice with phenol-chloroform. Finally, the DNA was precipitated by adding 1/10 volume 3 M sodium acetate (pH 5.0) and two volumes of absolute ethanol at –20°C. After the pellet was washed with 70% ethanol, it was dissolved in TE buffer (0.01 M Tris, 0.001 M EDTA, pH 7.5). Restriction site mapping was performed by digesting with the restriction enzyme HaeIII (Promega) according to the manufacturer's instructions. Fragments were separated by electrophoresis on a 7.5% polyacrylamide gel for 2 h at 70 V using the GeneRuler 1 kb DNA ladder (Fermentas) as a marker. PCR amplification of the putative DNA and RNA polymerases and exonuclease was performed using the following oligonucleotides: TACA GACTATGCCCTGCTG and AGTCTGTGGTGGATGATACC as the forward and reverse primer for DNA polymerase; CGT CAGTGGTACACAAAGG and GTGCAGCTACGTAATGTGG for RNA polymerase; and GTTAAGACGTTGCCTACTGC and CATAAGGTAGGCGTATCCAG for exonuclease. The primers were designed from the sequence obtained for the VP93 genome. PCR product sequences were deposited as FJ896201–FJ896221. The host range of the phages was determined by standard spot tests (Ceyssens *et al*., 2006).

Growth curves and phage persistence assays

A one-step growth curve was made by infecting an early exponential culture of *V. parahaemolyticus* PMC 57.5 with the phage at a moi of 10. The absorbance was monitored and samples were obtained at short time intervals for the determination of pfu and cfu. The pfu was determined after treatment with chloroform; plating was performed using the standard double-layer agar plaque assay. The cfu was determined by plating in soft agar using a described modified pour-plate method (Berney *et al*., 2006). Phage persistence in infected cultures was determined by 1:100 dilution of the stationary-phase cultures in fresh medium and continuing the incubation. Dilution and subsequent incubation until the stationary phase was performed four times in series. The pfu and cfu were determined after each serial culture reached stationary phase. Phage associated with cells in the last serial culture was determined by measuring the pfu after pelleting and washing the bacteria five times with the same volume of medium. The fraction of resistant cells in colonies was determined by plating the bacterial suspensions from each colony in solid medium with and without VP93. The VP93 adsorption rate was measured as described by Mudgal and colleagues (2006), except free phage was measured after centrifugation instead of filtration.

The presence of the phage genome in resistant bacteria was determined by testing for the presence of the putative RNA and DNA phage polymerase genes of VP93 in the bacteria from each of 20 colonies obtained from infected cultures after two passages (re-picked) in solid medium. The putative RNA and DNA phage polymerase genes of VP93 were assayed by PCR as described above. Positive controls for phage detection consisted of bacteria spiked with 0.01 pfu of VP93 per bacteria. The gene *tdh* of pandemic *V. parahaemolyticus* was amplified as a control for PCR amplification. Mitomycin C treatment was performed by adding fresh solution to obtain a final concentration of 30 ng ml^{-1} as previously described (Oakey *et al*., 2002).

Population dynamics

The bacterial and bacteriophage population dynamics were modelled as described by Levin and Bull (2004). The following algorithm was used with the indicated parameters:

```
{Lytic Phage with phase shifting – and mutation to Inherited
Resistance with VP93 parameters Initial infection}
{method definition}

METHOD EULER
starttime   = 0
STOPTIME    = 2.1
DT          = 0.0001
DTOUT       = 0.01

{Constant Parameters}

v           = 2.0 {Maximum growth rate sensitive S}
v1          = 2.0 {Maximum growth rate resistant R1}
v2          = 2.0 {Maximum growth rate resistant}
d1          = 1e-8 {Maximum adsorption rate parameter}
b1          = 1000 {Burst size}
k           = 0.25 {Monod coefficient}
e           = 5e-7 {Conversion efficiency}
mutR1S      = 1e-2 {Rate at which S cells produced R1}
mutSR1      = 1e-2 {Rate at which R1 produce S}
mu          = 1e-10 {Mutation rate to resistance S and to
              NR}
x           = 0.3 {Latent period}
m           = 1e-3 {Rate mortality P1}

{Variables}

init S      = 2.3e7 {Initial density of sensitive bacteria}
init R1     = 2.3e7 {Initial density of phenotypically
              resistant – phase shift bacteria}
init MS     = 0 {Initial density of infected S bacteria}
init NR     = 0 {Initial density of resistant bacteria}
init P      = 1e9 {Initial density of the phage}
init G      = 500 {Initial resource}
n           = s + r1
psi         = G/(k + G)
b           = b1*psi
d           = d1*psi

{Delay Variables}

Sx          = DELAY(S,x) {Sensitive at t – x}
R1x         = DELAY(R1,x) {R1 at t – x}
MSx         = DELAY(MS,x) {S infected with P at t – x}
Px          = DELAY(P,x) {P1 phage at t – x}

{Equations}

d/dt (G)    = –psi*e*(S*v + NR*v2 + R1*v1)
d/dt (S)    = (1 – mutR1S)*v*S*psi – d*S*P + mutSR1*
              R1*psi
```

d/dt (R1) = (1 – mutSR1)*v1*R1*psi + mutR1S*S*psi
d/dt (MS) = d*S*P
d/dt (NR) = v2*psi*NR + GM/dt
d/dt (P) = MSx*b – m*P

{Mutation}

bm = N*mu*DT
rm = RANDOM (0, 1)
GM = IF rm < bm THEN 1 ELSE 0

The same equations were used to model 1/100 dilutions, except that initial P, S and R1 were those corresponding to the 1/100 dilution of the previous culture and that STOPTIME was 16.

VP93 genome sequencing

Sequencing was performed as described above using the VP93 genome after cloning with the TOPO Shotgun Subcloning Kit (Invitrogen) as described by the manufacturer. Macrogen (Seoul, Korea) sequenced 161 clones (Seoul, Korea) using M13 forward and reverse primers. Seventeen contigs were obtained and gaps, direct repeats and uncertainties in the sequence were determined by direct sequencing of the phage genome using appropriate primers. Total sites determined corresponded to a 4.6-fold coverage of the genome. Sequence assembly was performed using the programs in the Staden Package (http://staden.sourceforge.net/). The genome sequence was scanned for potential ORFs using Artemis (http://www.sanger.ac.uk/Software/Artemis/) (Rutherford *et al*., 2000). Translated ORF sequences were compared with known proteins using standard protein–protein BLASTP (http://blast.ncbi.nlm.nih.gov/) (Altschul *et al*., 1990).

Acknowledgements

It is a pleasure to thank Pedro Romero from the Instituto de Biotecnología of Universidad Autónoma de México and Fernando Puerto from the Instituto Hidegeo Niguchi of Universidad de Yucatán for help isolating the bacteriophages from México. We thank Daniel Castillo and Camila Soriano for doing part of the modelling and most of the calculation. Roberto Bastías acknowledges scholarship from Programa MECE Educación Superior, proyecto UCH 0407. This work was partially supported by Grant FONDECYT 1076054.

References

Alam, M.J., Miyoshi, S., and Shinoda, S. (2003) Studies on pathogenic *Vibrio parahaemolyticus* during a warm weather season in the Seto Inland Sea, Japan. *Environ Microbiol* **5:** 706–710.

Altschul, S.F., Gish, W., Miller, W., Myers, E.W., and Lipman, D.J. (1990) Basic local alignment search tool. *J Mol Biol* **215:** 403–410.

Barksdale, L., and Arden, S.B. (1974) Persisting bacteriophage infections, lysogeny, and phage conversions. *Annu Rev Microbiol* **28:** 265–299.

Baross, J.A., Liston, J., and Morita, R.Y. (1978) Incidence of *Vibrio parahaemolyticus* bacteriophages and other *Vibrio* bacteriophages in marine samples. *Appl Environ Microbiol* **36:** 492–499.

Berney, M., Weilenmann, H.U., Ihssen, J., Bassin, C., and Egli, T. (2006) Specific growth rate determines the sensitivity of *Escherichia coli* to thermal, UVA, and solar disinfection. *Appl Environ Microbiol* **72:** 2586–2593.

Bouvier, T., and Giorgio, P.A. (2007) Key role of selective viral-induced mortality in determining marine bacterial community composition. *Environ Microbiol* **9:** 287–297.

Breitbart, M., and Rohwer, F. (2005) Here a virus, there a virus, everywhere the same virus? *Trends Microbiol* **13:** 278–284.

Brussaard, C.P., Wilhelm, S.W., Thingstad, F., Weinbauer, M.G., Bratbak, G., Heldal, M., *et al.* (2008) Global-scale processes with a nanoscale drive: the role of marine viruses. *ISME J* **2:** 575–578.

Brüssow, H., Canchaya, C., and Hardt, W.D. (2004) Phages and the evolution of bacterial pathogens: from genomic rearrangements to lysogenic conversion. *Microbiol Mol Biol Rev* **68:** 560–602.

Carey-Smith, G.V., Billington, C., Cornelius, A.J., Hudson, J.A., and Heineman, J.A. (2006) Isolation and characterization of bacteriophages infecting *Salmonella* spp. *FEMS Microbiol Lett* **258:** 182–186.

Ceyssens, P.J., Lavigne, R., Mattheus, W., Chibeu, A., Hertveldt, K., Mast, J., *et al.* (2006) Genomic analysis of *Pseudomonas aeruginosa* phages LKD16 and LKA1: establishment of the phiKMV subgroup within the T7 supergroup. *J Bacteriol* **188:** 6924–6931.

Comeau, A.M., Buenaventura, E., and Suttle, C.A. (2005) A persistent, productive, and seasonally dynamic vibriophage population within Pacific oysters (*Crassostrea gigas*). *Appl Environ Microbiol* **71:** 5324–5331.

Comeau, A.M., Chan, A.M., and Suttle, C.A. (2006) Genetic richness of vibriophages isolated in a coastal environment. *Environ Microbiol* **8:** 1164–1176.

Depaola, A., Kaysner, C.A., Bowers, J., and Cook, D.W. (2000) Environmental investigations of *Vibrio parahaemolyticus* in oysters after outbreaks in Washington, Texas, and New York (1997 and 1998). *Appl Environ Microbiol* **66:** 4649–4654.

Depaola, A., Nordstrom, J.L., Bowers, J.C., Wells, J.G., and Cook, D.W. (2003a) Seasonal abundance of total and pathogenic *Vibrio parahaemolyticus* in Alabama oysters. *Appl Environ Microbiol* **69:** 1521–1526.

Depaola, A., Ulaszek, J., Kaysner, C.A., Tenge, B.J., Nordstrom, J.L., Wells, J., *et al.* (2003b) Molecular, serological, and virulence characteristics of *Vibrio parahaemolyticus* isolated from environmental, food, and clinical sources in North America and Asia. *Appl Environ Microbiol* **69:** 3999–4005.

Enos-Berlage, J.L., and McCarter, L.L. (2000) Relation of capsular polysaccharide production and colonial cell organization to colony morphology in *Vibrio parahaemolyticus*. *J Bacteriol* **182:** 5513–5520.

Fischer, C.R., Yoichi, M., Unno, H., and Tanji, Y. (2004) The coexistence of *Escherichia coli* serotype O157 : H7 and its specific bacteriophage in continuous culture. *FEMS Microbiol Lett* **241:** 171–177.

Fuenzalida, L., Hernandez, C., Toro, J., Rioseco, M.L., Romero, J., and Espejo, R.T. (2006) *Vibrio parahaemolyti-*

cus in shellfish and clinical samples during two large epidemics of diarrhoea in southern Chile. *Environ Microbiol* **8:** 675–683.

Hara-Kudo, Y., Sugiyama, K., Nishibuchi, M., Chowdhury, A., Yatsuyanagi, J., Ohtomo, Y., *et al.* (2003) Prevalence of pandemic thermostable direct hemolysin-producing *Vibrio parahaemolyticus* O3 : K6 in seafood and the coastal environment in Japan. *Appl Environ Microbiol* **69:** 3883–3891.

Hardies, S.C., Comeau, A.M., Serwer, P., and Suttle, C.A. (2003) The complete sequence of marine bacteriophage VpV262 infecting *Vibrio parahaemolyticus* indicates that an ancestral component of a T7 viral supergroup is widespread in the marine environment. *Virology* **310:** 359–371.

Iida, T., Hattori, A., Tagomori, K., Nasu, H., Naim, R., and Honda, T. (2001) Filamentous phage associated with recent pandemic strains of *Vibrio parahaemolyticus*. *Emerg Infect Dis* **7:** 477–478.

Izutsu, K., Kurokawa, K., Tashiro, K., Kuhara, S., Hayashi, T., Honda, T., and Iida, T. (2008) Comparative genomic analysis using microarray demonstrates a strong correlation between the presence of the 80-kilobase pathogenicity island and pathogenicity in Kanagawa phenomenon-positive *Vibrio parahaemolyticus* strains. *Infect Immun* **76:** 1016–1023.

Koga, T., and Kawata, T. (1991) Comparative characterization of inducible and virulent *Vibrio parahaemolyticus* bacteriophages having unique head projections. *Microbiol Immunol* **35:** 49–58.

Kudriakova, T., Makedonova, L.D., Dudkina, O.S., Degtiarev, B.M., Khaitovich, A.B., Savchenko, B.I., *et al.* (1992) The phages of halophilic vibrios and its use. *Zh Mikrobiol Epidemiol Immunobiol* **9–10:** 5–7 (in Russian).

Lan, S.F., Huang, C.H., Chang, C.H., Liao, W.C., Lin, I.H., Jian, W.N., *et al.* (2009) Characterization of a new plasmid-like prophage in a pandemic *Vibrio parahaemolyticus* O3 : K6 strain. *Appl Environ Microbiol* **75:** 2659–2667.

Levin, B.R., and Bull, J.J. (2004) Population and evolutionary dynamics of phage therapy. *Nat Rev Microbiol* **2:** 166–173.

Makino, K., Oshima, K., Kurokawa, K., Yokoyama, K., Uda, T., Tagomori, K., *et al.* (2003) Genome sequence of *Vibrio parahaemolyticus*: a pathogenic mechanism distinct from that of *V cholerae*. *Lancet* **361:** 743–749.

Matsuzaki, S., Inoue, T., Tanaka, S., Koga, T., Kuroda, M., Kimura, S., and Imai, S. (2000) Characterization of a novel *Vibrio parahaemolyticus* phage, KVP241, and its relatives frequently isolated from seawater. *Microbiol Immunol* **44:** 953–956.

Middelboe, M., Holmfeldt, K., Riemann, L., Nybroe, O., and Haaber, J. (2009) Bacteriophages drive strain diversification in a marine *Flavobacterium*: implications for phage resistance and physiological properties. *Environ Microbiol* **11:** 1971–1982.

Miller, E.S., Heidelberg, J.F., Eisen, J.A., Nelson, W.C., Durkin, A.S., Ciecko, A., *et al.* (2003) Complete genome sequence of the broad-host-range vibriophage KVP40: comparative genomics of a T4-related bacteriophage. *J Bacteriol* **185:** 5220–5233.

Mudgal, P., Breidt, F., Jr, Lubkin, S.R., and Sandeep, K.P. (2006) Quantifying the significance of phage attack on starter cultures: a mechanistic model for population dynamics of phage and their hosts isolated from fermenting sauerkraut. *Appl Environ Microbiol* **72:** 3908–3915.

Muramatsu, K., and Matsumoto, H. (1991) Two generalized transducing phages in *Vibrio parahaemolyticus* and *Vibrio alginolyticus*. *Microbiol Immunol* **35:** 1073–1084.

Nair, G.B., Ramamurthy, T., Bhattacharya, S.K., Dutta, B., Takeda, Y., and Sack, D.A. (2007) Global dissemination of *Vibrio parahaemolyticus* serotype O3 : K6 and its serovariants. *Clin Microbiol Rev* **20:** 39–48.

Nasu, H., Iida, T., Sugahara, T., Yamaichi, Y., Park, K.S., Yokoyama, K., *et al.* (2000) A filamentous phage associated with recent pandemic *Vibrio parahaemolyticus* O3 : K6 strains. *J Clin Microbiol* **38:** 2156–2161.

Oakey, H.J., Cullen, B.R., and Owens, L. (2002) The complete nucleotide sequence of the *Vibrio harveyi* bacteriophage VHML. *J Appl Microbiol* **93:** 1089–1098.

Ogura, Y., Kurokawa, K., Ooka, T., Tashiro, K., Tobe, T., Ohnishi, M., *et al.* (2006) Complexity of the genomic diversity in enterohemorrhagic *Escherichia coli* O157 revealed by the combinational use of the O157 Sakai OligoDNA microarray and the Whole Genome PCR scanning. *DNA Res* **13:** 3–14.

Ohnishi, T., and Nozu, K. (1986) Induction of phage-like particles from a pathogenic strain of *Vibrio parahaemolyticus* by mitomycin C. *Biochem Biophys Res Commun* **141:** 1249–1253.

Rutherford, K., Parkhill, J., Crook, J., Horsnell, T., Rice, P., Rajandream, M.A., and Barrell, B. (2000) Artemis: sequence visualization and annotation. *Bioinformatics* **16:** 944–945.

Sumby, P., and Smith, M.C. (2003) Phase variation in the phage growth limitation system of *Streptomyces coelicolor* A3(2). *J Bacteriol* **185:** 4558–4563.

Suttle, C.A. (2005) Viruses in the sea. *Nature* **437:** 356–361.

Wommack, K.E., and Colwell, R.R. (2000) Virioplankton: viruses in aquatic ecosystems. *Microbiol Mol Biol Rev* **64:** 69–114.

Zabala, B., Garcia, K., and Espejo, R.T. (2009) Enhancement of UV light sensitivity of a *Vibrio parahaemolyticus* O3 : K6 pandemic strain due to natural lysogenization by a telomeric phage. *Appl Environ Microbiol* **75:** 1697–1702.

Zaleski, P., Wojciechowski, M., and Piekarowicz, A. (2005) The role of Dam methylation in phase variation of *Haemophilus influenzae* genes involved in defence against phage infection. *Microbiology* **151:** 3361–3369.

Supporting information

Additional Supporting Information may be found in the online version of this article:

Fig. S1. Dendrogram illustrating the pattern clusters based on the dissimilarity of the nucleotide sequences in PCR amplicons of the putative genes for DNA and RNA polymerases and exonuclease. Line 0.1 corresponds to changes per nucleotide position.

Table S1. Infectivity of phage isolates from different RFLP clusters on diverse *V. parahaemolyticus* strains. Isolates not shown were not included in the present analysis.

Table S2. Sequence of regions around essential catalytic residues of RNA polymerase. Conserved residues with phage VP93 are in bold. The essential catalytic residues are underlined.